THE JOURNAL OF BIOLOGICAL CHEMISTRY VOL. 288, NO. 26, pp. 18673–18683, June 21, 2013

Structural Insights into Aβ42 Oligomers Using Site-directed Spin Labeling*◆

Received for publication, January 30, 2013, and in revised form, April 29, 2013 Published, JBC Papers in Press, May 16, 2013, DOI 10.1074/jbc.M113.457739

Lei Gu‡, Cong Liu§, and Zhefeng Guo‡1

From the ‡Department of Neurology, Brain Research Institute, Molecular Biology Institute and the §UCLA-DOE Institute for Genomics and Proteomics, UCLA, Los Angeles, California 90095

Background: Aβ42 oligomers underlie neurotoxicity in Alzheimer disease, but their molecular structures are unknown.
Results: Electron paramagnetic resonance studies reveal intermolecular distances at 11.5–12.5 Å for C-terminal region of Aβ42.
Conclusion: Aβ42 oligomers consist of a tightly packed C-terminal region that adopts antiparallel structures.
Significance: This work provides insights into the structures of Aβ42 oligomers and helps understand their oligomerization mechanism and toxicity.

Oligomerization of the 42-residue peptide Aβ42 plays a key role in the pathogenesis of Alzheimer disease. Despite great academic and medical interest, the structures of these oligomers have not been well characterized. Site-directed spin labeling combined with electron paramagnetic resonance spectroscopy is a powerful approach for studying structurally ill-defined systems, but its application in amyloid oligomer structure study has not been systematically explored. Here we report a comprehensive structural study on a toxic Aβ42 oligomer, called globulomer, using site-directed spin labeling complemented by other techniques. Transmission electron microscopy shows that these oligomers are globular structures with diameters of ~7–8 nm. Circular dichroism shows primarily β-structures. X-ray powder diffraction suggests a highly ordered intrasheet hydrogen-bonding network and a heterogeneous intersheet packing. Residue-level mobility analysis on spin labels introduced at 14 different positions shows a structured state and a disordered state at all labeling sites. Side chain mobility analysis suggests that structural order increases from N- to C-terminal regions. Intermolecular distance measurements at 14 residue positions suggest that C-terminal residues Gly-29–Val-40 form a tightly packed core with intermolecular distances in a narrow range of 11.5–12.5 Å. These intermolecular distances rule out the existence of fibril-like parallel in-register β-structures and strongly suggest an antiparallel β-sheet arrangement in Aβ42 globulomers.

Aggregation of amyloid β (Aβ)[2] peptide is a key event in the pathogenesis of Alzheimer disease (AD) (1). Aβ is the proteolytic product of amyloid precursor protein by the sequential cleavages of β- and γ-secretases (2). There are two major Aβ isoforms: Aβ42 (42 residues long) and Aβ40 (40 residues long). Aβ42 differs from Aβ40 by having two additional C-terminal residues. Although Aβ40 is severalfold more abundant than Aβ42 in the brain, Aβ42 is the major component in AD plaques (3), suggesting that the aggregation of Aβ42 precedes Aβ40. Aggregation of Aβ results in the formation of insoluble amyloid fibrils, soluble oligomers, and protofibrils. In recent years, AD research has shifted from a fibril-centric to an oligomer-centric view, reflecting the good correlation between soluble Aβ oligomers and AD progression (4, 5). A number of oligomeric Aβ assemblies have been identified *in vivo* and *in vitro*. Oligomer formation has also been found in other amyloid-related disorders, suggesting that oligomer-induced toxicity may be a common mechanism for a range of protein misfolding diseases (6).

Different Aβ oligomers such as dimers (7, 8), trimers (9), and Aβ*56 (9) have been identified in AD brains, transgenic AD model animals, or cultured cells. Various protocols have also been devised to stabilize and enrich Aβ oligomers in the test tube (10, 11). Antibodies have been generated using several of these oligomer preparations including Aβ-derived diffusible ligands (12), globulomers (13), prefibrillar oligomers (14), and amylospheroids (15). Positive staining has been found in AD brain slices using these antibodies, suggesting that these Aβ oligomers are related to endogenous Aβ assemblies. Without the atomic-level structural information of these Aβ oligomers, it is impossible to know how many unique structures are present in these oligomers. The general lack of cross-reactivity among different oligomer-specific antibodies suggests that the surface-exposed groups are distinct in different oligomer preparations. On the other hand, similar structural features have also been found, which include β-strand structures at the central hydrophobic cluster (residues 17–20) and the C-terminal hydrophobic region (residues 30–40) and a turn/loop structure at residues 20–30. Antiparallel arrangement between β-strands has also been suggested based on Fourier transform infrared (FTIR) studies of Aβ oligomers prepared using a range of protocols (16–24).

Detailed structural studies of these Aβ oligomers are urgently needed for several reasons. First, Aβ oligomers are toxic species and thus represent drug targets in AD. Second, structural knowledge is critical for understanding the structural

* This work was supported by the Alzheimer's Association (Grant NIRG-09-133555) and American Health Assistance Foundation (Grant A2010362).
◆ This article was selected as a Paper of the Week.
[1] To whom correspondence should be addressed: Dept. of Neurology, UCLA, 710 Westwood Plaza, Los Angeles, CA 90095. Tel.: 310-206-8773; E-mail: zhefeng@ucla.edu.
[2] The abbreviations used are: Aβ, amyloid β; AD, Alzheimer disease; TEM, transmission electron microscopy; SEC, size exclusion chromatography; HFIP, 1,1,1,3,3,3-hexafluoro-2-propanol; MTT, 3-(4,5-dimethylthiazol-2-yl)-2,5-diphenyltetrazolium bromide; DMSO, dimethyl sulfoxide.

basis of Aβ toxicity and the mechanism of aggregation. Third, detailed structural studies will help to determine whether each *in vitro* oligomer preparation can be assigned a unique structural identity. High-resolution structural studies on peptide fragments and macrocyclic β-sheet mimics have provided insights into the potential organization of amyloid oligomers (25, 26). However, detailed structures of full-length Aβ oligomers still remain elusive.

To this end, we performed a comprehensive structural study on a toxic Aβ42 oligomer termed globulomer (13) using site-directed spin labeling and electron paramagnetic resonance (EPR) spectroscopy (27–31). Globulomers are a relatively stable and homogeneous preparation of Aβ oligomers, and they do not convert to fibrils (32). Endogenous Aβ globulomers are detected in the brain by globulomer-specific antibodies (13, 33). Previous studies suggest that globulomers are dodecamers and show synaptic toxicity (13, 33, 34). Solution NMR studies on preglobulomers show that they contain both antiparallel and parallel structures (35), but the detailed structures of globulomers are still unknown.

In this work, we demonstrate that Aβ42 forms globular oligomers revealed by transmission electron microscopy (TEM), which are toxic to mammalian cell lines. Circular dichroism (CD) and x-ray powder diffraction show that these oligomers consist of cross-β-structures. We then performed site-directed spin labeling EPR studies on the Aβ42 globulomers with spin labels introduced, one at a time, at 14 different residue positions throughout the Aβ42 sequence. Spin label mobility analysis shows increasing structural order from N- to C-terminal regions. Distance measurements reveal that intermolecular distances for most labeling sites are in the range of 11.5–13.5 Å in the oligomers. These measured distances indicate a tightly packed C-terminal region and a loosely packed N-terminal region. These distances also suggest that Aβ42 globulomers adopt antiparallel β-structures.

EXPERIMENTAL PROCEDURES

Preparation of Aβ42 Peptides and Spin Labeling—The DNA construct of GroES-ubiquitin-Aβ42 (36) and the deubiquitylating enzyme Usp2cc (37) were kindly provided by Dr. Rohan T. Baker at Australian National University (Australia) and Dr. Il-Seon Park at Chosun University (South Korea). Single cysteine mutations at various sites were introduced into Aβ42 sequence using a QuikChange kit (Agilent). Mutations were confirmed with DNA sequencing.

Expression of GroES-ubiquitin-Aβ42 and Usp2cc proteins in *Escherichia coli* and their purification were performed as described previously (28, 38). Full-length Aβ42 was cleaved from the fusion protein with Usp2cc. The enzymatic digestion was performed in a buffer containing 19 mM phosphate, 3 M urea, 2 mM tris(2-carboxyethyl)phosphine, pH 10.0. Usp2cc was added to the fusion protein at a molar ratio of 1:100. The digestion reaction was allowed to proceed at 37 °C for 15 min. The reaction mixture was then immediately filtered with a 0.2-μm filter (Whatman) and loaded on a 5-ml HisTrap column (GE Healthcare) equilibrated with PSU buffer (50 mM phosphate, 0.3 M NaCl, 8 M urea, pH 10.0). Aβ42 protein was eluted using a gradient of 25 mM imidazole. Purified Aβ42 was checked with SDS-PAGE, and no uncleaved proteins were detected.

For spin labeling, dithiothreitol was added to purified protein fraction to a final concentration of 10 mM and was allowed to incubate at room temperature for 20 min to break any disulfide bonds. Then the Aβ42 sample was buffer-exchanged to labeling buffer (20 mM MOPS, 7 M guanidine hydrochloride, 50 mM NaCl, pH 6.8) using a 5-ml HiTrap desalting column (GE Healthcare). The spin labeling reagent 1-oxyl-2,2,5,5-tetramethylpyrroline-3-methyl methanethiosulfonate (Enzo Life Sciences) was added at 10 times molar excess and then incubated at room temperature for 1 h. The spin-labeled Aβ42 was further buffer-exchanged to 30 mM ammonium acetate, pH 10.0, lyophilized, and stored at −80 °C. MALDI-TOF mass spectrometry was performed to ensure that the mass of Aβ42 is correct and that the extent of labeling is >95%.

Preparation of Aβ42 Globulomer—Aβ42 oligomers were prepared using the globulomer protocol (35) with modifications. Aβ42 peptide was suspended in 100% 1,1,1,3,3,3-hexafluoro-2-propanol (HFIP) at 1 mM and then bath-sonicated for 5 min. Then the sample was incubated at room temperature for 30 min. HFIP was removed by evaporation overnight in the fume hood and then under vacuum for 1 h. HFIP-treated Aβ42 was resuspended in dimethyl sulfoxide at 5 mM and sonicated for 5 min. Then Aβ42 was diluted in phosphate-buffered saline (PBS) (20 mM phosphate, 140 mM NaCl, pH 7.4) to 400 μM, and sodium dodecyl sulfate (SDS) was added to a final concentration of 0.2%. After incubation for 6 h at 37 °C, Aβ42 samples were further diluted with 3 volumes of H_2O to a final concentration of 100 μM and incubated for another 18 h at 37 °C. After centrifugation at 14,000 × *g* for 20 min, the supernatant was concentrated by ultrafiltration using 30-kDa molecular mass cut-off filters.

Transmission Electron Microscopy—The Aβ42 oligomer sample (5 μl) was placed on glow-discharged copper grids covered with 400-mesh Formvar/carbon film (Ted Pella). The sample was negatively stained with 2% uranyl acetate. Samples were examined using a JEOL JEM-1200EX transmission electron microscope at 80 kV, and images were recorded using a top-mounted charge-coupled device camera (Gatan).

MTT-based Cell Viability Assays—3-(4,5-Dimethylthiazol-2-yl)-2,5-diphenyltetrazolium bromide (MTT)-based CellTiter 96 nonradioactive cell proliferation assay (Promega) was performed for a cell viability test. HeLa and PC-12 cell lines were used in the assay. Prior to the MTT test, PC-12 cells were cultured in ATCC-formulated RPMI 1640 medium (ATCC catalog number 30-2001) with 10% heat-inactivated horse serum and 5% fetal bovine serum at 37 °C in 5% CO_2, and HeLa cells were cultured in DMEM medium with 10% fetal bovine serum at 37 °C in 5% CO_2. HeLa and PC-12 cells were plated out at 10,000 cells/well in 96-well plates (Costar catalog number 3596) and cultured for 20 h at 37 °C in 5% CO_2. To initiate the test, 10 μl of sample was added into each well containing 90 μl of medium. After 24 h of incubation, 15 μl of dye solution (Promega catalog number G4000) was added into each well, and the mixture was further incubated for 4 h at 37 °C in 5% CO_2. Then 100 μl of solubilization solution/stop mix (Promega catalog number G4000) was added to each well with 12 h of incubation

at room temperature for complete solubilization of the dye crystals. The absorbance was measured at 570 nm. The background absorbance was recorded at 700 nm. The readout from buffer blank treated cell is regarded as 100% viability, and that from 0.2% treated cell is treated as 0% viability. Four replicates per sample were measured for calculating standard deviation.

Circular Dichroism—Secondary structures of Aβ42 samples were analyzed by CD spectroscopy. Samples (~40 μl) were placed into a 0.01-cm path length quartz cell (Starna). A JASCO J-715 CD spectrometer was employed. The measurements were carried out in a wavelength range of 190–260 nm at a rate of 20 nm/min with a step resolution of 0.5 nm, a time constant of 4 s, and a bandwidth of 1 nm. The CD spectra were obtained by averaging 16 scans. The temperature was set at 25 °C. All the spectra were corrected by subtracting the buffer background.

X-ray Powder Diffraction—Aβ42 oligomer was washed with H_2O using the 30-kDa molecular mass cut-off filter and lyophilized. The powder was mounted on the tip of a broken glass rod. Then, the specimen was placed on the goniometer of an in-house x-ray machine and shot using a Rigaku FR-D x-ray generator equipped with a Rigaku HTC imaging plate detector.

Analytical Size Exclusion Chromatography—The size of Aβ42 globulomer was analyzed by analytical SEC using a Superdex 200 10/300 GL column (GE Healthcare) attached to an ÄKTA explorer system (GE Healthcare). Prior to Aβ42 oligomer sample injection (50 μl), the column was washed with 2 column volumes of filtered, degassed globulomer buffer (5 mM phosphate, pH 7.4, 35 mM NaCl, 2% DMSO, and 0.05% SDS). The molecular mass of Aβ42 globulomer was estimated based on the SEC profiles of protein standards (Bio-Rad).

EPR Spectroscopy—EPR measurements were performed at X-band frequency on a Bruker EMX spectrometer equipped with the ER 4102ST cavity. A modulation frequency of 100 kHz was used. For measurements performed at room temperature, 20 milliwatts of microwave power was employed. EPR spectra of both the retentate and the filtrate after ultrafiltration with 30-kDa filter were collected. The filtrate component, accounting for <1% of total EPR signal, was subtracted from the retentate spectra to obtain the spectra of "pure" globulomers. For measurements performed at 170 K, 631 milliwatts of microwave power was used. Modulation amplitude was optimized to each individual spectrum. For each sample, 20 μl of solution was loaded into glass capillaries (VitroCom) sealed at one end. For measurements performed in frozen solution at 170 K, 20% (v/v) glycerol was added to the sample solution followed by flash-freezing the sample in liquid nitrogen. EPR spectra in each figure panel were normalized to the same number of spins.

Spectral Simulations and Distance Analysis—Spectral simulations were performed using the program MultiComponent (developed by Dr. Christian Altenbach, UCLA), which provides a LabVIEW interface for the program NLSL developed by Freed and co-workers (39, 40). A microscopic order/macroscopic disorder model was used for all simulations (40). A nonlinear least squares fit of the user-defined spectral parameters was performed using the Levenberg-Marquardt algorithm. For all fits, the values for the magnetic tensors A and g were fixed as A_{xx} = 6.2, A_{yy} = 5.9, A_{zz} = 37.0, and g_{xx} = 2.0078, g_{yy} = 2.0058, g_{zz} = 2.0022, which were determined previously for R1 (59). Each spectrum was fitted with two spectral components. The isotropic rotational diffusion constant (D) was allowed to vary for each component. The rotational correlation time (τ) was calculated from $\tau = 1/(6D)$. The values of τ and populations of each spectral component are plotted in Fig. 3. Local structural stability at each labeling site was calculated using $\Delta G = -RT\ln K$, where K is the ratio between the slow component population and the fast component population, while assuming the fast component represents the locally unfolded state.

Distance analysis was performed using the program Short-Distances (developed by Dr. Christian Altenbach, UCLA). The detailed fitting procedure to obtain distances has been previously described (41). The 25% labeled spectra were used as the spectra without dipolar interactions. The width of the distance distribution was fixed at 3 Å. The distance, percentage of the spin labels at the fitted distance, the percentage of noninteracting spin labels were allowed to vary. The best fits of these parameters are plotted in Fig. 5.

RESULTS

Characterization of Wild-type Aβ42 Globulomers—We prepared Aβ42 oligomers with a globulomer protocol (13), which uses low concentration of SDS (0.05%) to mimic the lipid environment in the cell (42). TEM shows that the oligomer preparation contains mostly globular structures (Fig. 1*A*). Most globular oligomers have diameters ranging from 5 to 10 nm, with the majority of them around 7–8 nm (Fig. 1*B*). Elongated structures with a beaded string morphology can also be observed. The morphologies are similar to previous atomic force microscopy studies on globulomers, which show heights of 4–5 nm (35). MTT-based cell survival assays show that these Aβ42 oligomers are toxic to both PC-12 neuronal cells and HeLa cells in a dose-dependent manner (Fig. 1*C*). Approximately 20% of the cells died in the presence of 0.2 μM (monomer equivalent) Aβ42 globulomers, and ~60% of cells died in the presence of 2 μM Aβ42 globulomers. The CD spectrum shows a major negative peak at 216–218 nm, indicative of mostly β-structures (Fig. 1*D*), and it is similar to Aβ42 fibrils (Fig. 1*D*). In comparison, the Aβ42 monomer shows a single large negative peak at around 198 nm, characteristic of random coil structures (Fig. 1*D*). X-ray powder diffraction reveals three major diffraction peaks at 4.2, 4.7, and 10 Å (Fig. 1*E*). The 4.7 Å reflection arises from the separation of strands within the same β-sheet. The peak at ~10 Å corresponds to separations between β-sheets. The diffuse nature of the 10 Å peak suggests high heterogeneity of the intersheet packing. The origin of the 4.2 Å reflection is not well understood. Previously, an x-ray powder diffraction study of porcine stomach mucin protein showed a 4.2 Å reflection corresponding to distorted antiparallel β-structures (43), suggesting that similar structures may be present in Aβ42 globulomers. A SEC profile shows that the globulomers contain a major peak with a molecular mass of ~100–150 kDa (Fig. 1*F*). A minor peak at >700 kDa likely corresponds to the species with beaded string morphology under TEM (Fig. 1*A*). SEC also shows that Aβ42 globulomers do not contain a significant amount of monomer or small oligomers (Fig. 1*F*).

Preparation of Spin-labeled Aβ42 Globulomers for EPR Study—To study the structure of Aβ42 globulomers by EPR, we intro-

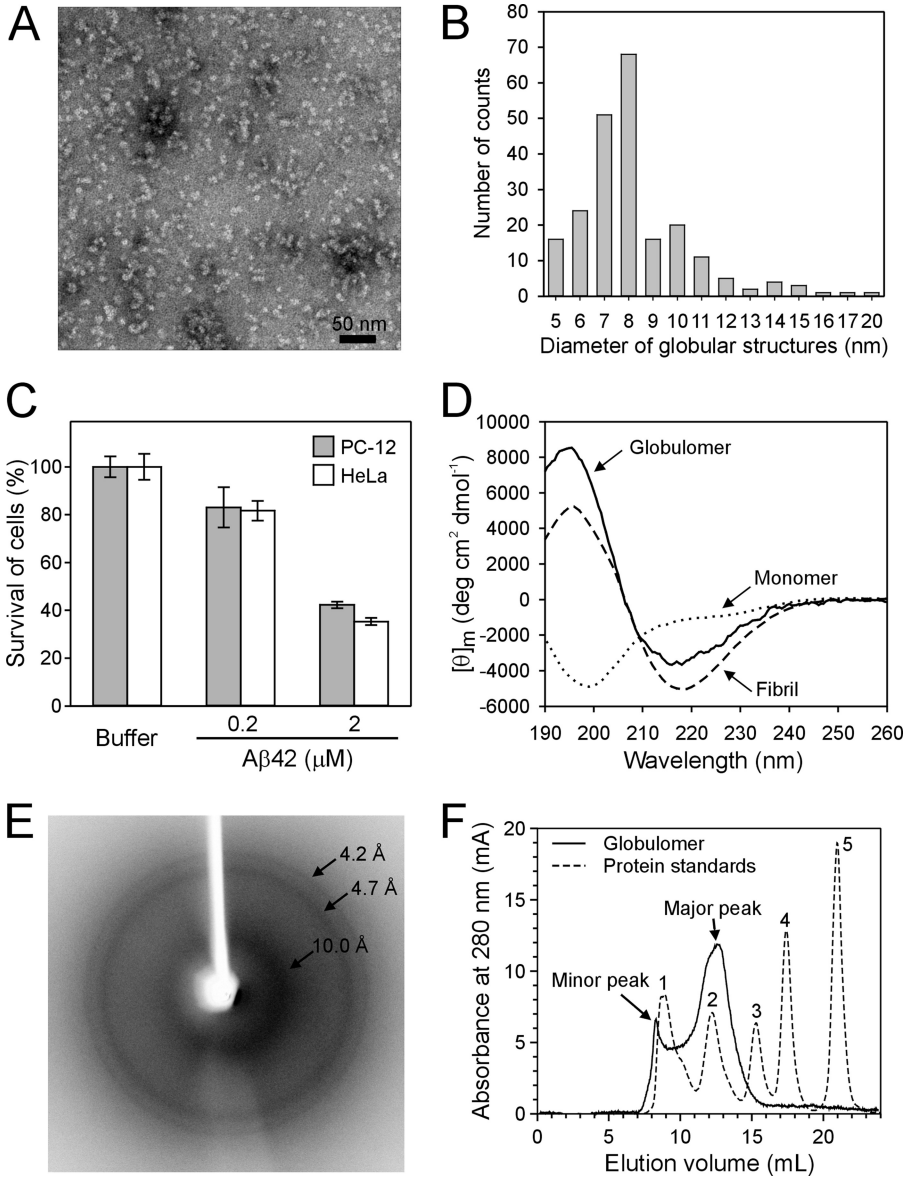

FIGURE 1. **Characterization of wild-type Aβ42 globulomers.** *A*, TEM image of Aβ42 globulomers. *B*, diameters of Aβ42 globulomers from TEM studies. *C*, survival of PC-12 and HeLa cells in the presence of Aβ42 globulomers using MTT-based cell viability assay. The buffer control has the exact composition as in the final step of globulomer preparation. *Error bars* indicate S.D. *D*, CD measurement of Aβ42 globulomers, fibrils, and monomers. A major negative peak at 216–218 nm suggests that Aβ42 globulomers contain predominantly β-structures. *E*, x-ray powder diffraction of lyophilized Aβ42 globulomers. *F*, analytical size exclusion chromatography profile of Aβ42 globulomers. *Solid trace*, globulomers; *dotted trace*, protein standards. The molecular masses of protein standards are: *peak 1*, thyroglobulin, 670 kDa; *peak 2*, bovine γ-globulin, 158 kDa; *peak 3*, chicken ovalbumin, 44 kDa; *peak 4*, equine myoglobin, 17 kDa; *peak 5*, vitamin B12, 1.35 kDa.

duced spin labels, one at a time, at 14 residue positions throughout the Aβ42 sequence (Fig. 2*A*). The spin label side chain used in this study is named R1 (Fig. 2*B*). TEM studies on selected spin-labeled Aβ42 globulomer samples show mostly globular structures without fibrils or protofibrils (Fig. 2*C*), suggesting that spin labeling does not significantly perturb the formation of Aβ42 globulomers.

Spin Label Mobility Analysis in Aβ42 Globulomers—The EPR spectra of spin-labeled Aβ42 globulomers are shown in Fig. 3*A* (*black traces*). For spin label mobility analysis, we prepared the oligomers using a mixture of spin-labeled Aβ42 with wild-type Aβ42 at 1:3 molar ratio. Therefore, in the oligomer sample, only 25% of the Aβ42 molecules were labeled, and this will greatly reduce dipolar interactions between spin labels. Spin-spin interactions may broaden the EPR spectra and complicate the mobility analysis.

The site-specific spin label mobility is an indicator of residue-level structural order (44). The EPR spectra of spin-labeled Aβ42 globulomers encode information about the mobility of the spin label at each labeling site. The spin label mobility can be measured using center line width (45) or the ratio of high field and center line amplitude (46). For EPR spectra with multiple components reflecting multiple motional states of the spin label, however, these measurements report only the combined mobility from different spin label states. A quantitative method to extract mobility information is spectral simulation. Multiple spectral components can be simulated simultaneously, and the

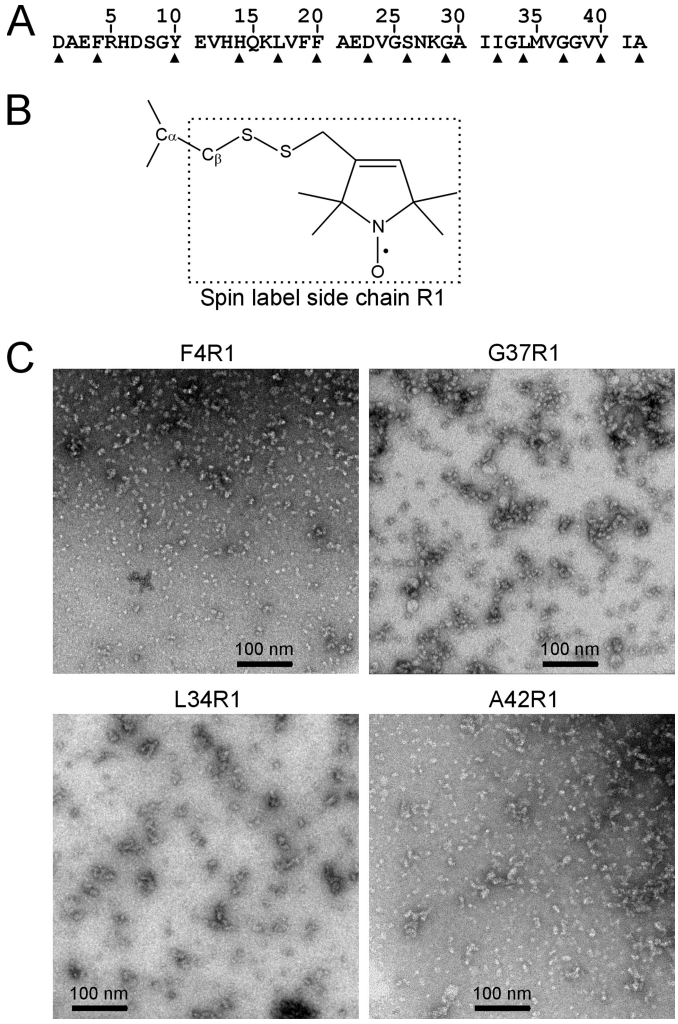

FIGURE 2. **Globulomers of spin-labeled Aβ42.** *A*, amino acid sequence of Aβ42 with spin labeling positions shown with *arrowheads*. *B*, structure of the spin label side chain R1 used in this work. *C*, TEM images of four representative spin-labeled Aβ42 globulomers show globular structures as major species.

population of each component can be obtained from simulation (47). Therefore, we performed nonlinear least squares fitting to the EPR spectra using spectral simulation (see "Experimental Procedures"). The best fits are shown in Fig. 3*A* (*red traces*). Spectral fitting revealed two spectral components at every spin labeling position: a fast component and a slow component (Fig. 3*A*, *magenta* and *blue traces*).

The presence of two spectral components suggests that globulomers contain at least two structural states whose interconversion is slower than the nanosecond timescale. The slow component has a correlation time of 2.0–3.0 ns in the N-terminal region and 3.0–4.5 ns in the C-terminal region, corresponding to a structured state. Spin labels at positions 1 and 4 have correlation time of ~2.1 ns. Although they are the most flexible region in the Aβ42 sequence, the spin label mobility at these residues is comparable with ordered helix surface sites (44) or solvent-exposed β-sheet sites (48, 49). Therefore, the EPR data suggest that the N-terminal region adopts some ordered structures. The structural order increases from N terminus to C terminus. The most ordered region spans residues 32–40, with a correlation time between 3.5 and 4.5 ns. These residues have spin label mobility comparable with spin labels located in the hydrophobic core of globular proteins (50).

The correlation time of the fast component is in the range of 0.7–1.7 ns, with decreasing side chain mobility from N- to C-terminal regions (Fig. 3*B*). Spin labels in completely unfolded proteins have a correlation time of ~0.5 ns (46, 47), suggesting that this fast component corresponds to a partly disordered state. The relative population of the fast component is ~25% for N-terminal region (residues 1–10) and 10–15% for most other residues (Fig. 3*C*), suggesting that the fast component represents a locally disordered state rather than a disordered monomer. This notion is further supported by the absence of a significant amount of monomer or small oligomer peaks in the SEC profile (Fig. 1*F*).

The residue-level local stability can be calculated with the assumption that the structured state (corresponding to the slow component) and the locally disordered state (corresponding to the fast component) are in equilibrium. The free energy of local unfolding in Aβ42 globulomers is calculated using the percentages of slow and fast components from simulation (Fig. 3*D*). This local stability plot reveals three low stability regions: Asp-1–Tyr-10, Ser-26–Gly-29, and Gly-37. The low stability at residue Gly-37 supports a likely turn structure at this position.

We investigated the temporal stability of Aβ42 globulomers using the spin label as a structural probe. The EPR spectral line shape of Aβ42 globulomers spin-labeled at residue 34 remains extremely similar upon incubation at room temperature (~21 °C) for 0, 4, 8, 24, and 48 h (Fig. 4*A*), suggesting no structural changes during this incubation period. The results also show that there are no structural changes during EPR measurements, which typically take less than 20 min.

Next we studied the temporal stability of Aβ42 globulomers upon dilution into cell culture medium. Following a 10-fold dilution to RPMI 1640 medium, the EPR spectral line shape of Aβ42 globulomer remains largely the same, consisting of two spectral components (Fig. 4*B*). The line shape of both the ordered and the disordered components remains unchanged upon incubation at room temperature for 0, 4, 8, 24, and 48 h. The only change is the relative population of the two components, with the disordered component increasing slightly from ~3.7% at 0 h to ~5.5% at 48 h.

Intermolecular Distance Measurements in Aβ42 Globulomers—To measure interspin distances using spin-spin interactions, we prepared globulomers using only spin-labeled Aβ42 (*i.e.* 100% labeled). Fig. 5*A* shows that the spectral amplitude of the 100% labeled sample (*red traces*) is reduced when compared with the 25% labeled sample (*black traces*), suggesting the existence of dipolar interactions. It should be noted that the EPR spectral line shape of the 100% labeled Aβ oligomer is dramatically different from the 100% labeled Aβ fibrils (28). In the parallel in-register β-structure of Aβ fibrils, spin labels are stacked on top of each other, giving rise to a single-line spectrum characteristic of strong spin exchange interactions (28). Clearly, the EPR spectra of the 100% labeled oligomers are indicative of dipolar interactions and do not have the single-line feature. Therefore, EPR data suggest that Aβ42 globulomers adopt structures different from fibrils.

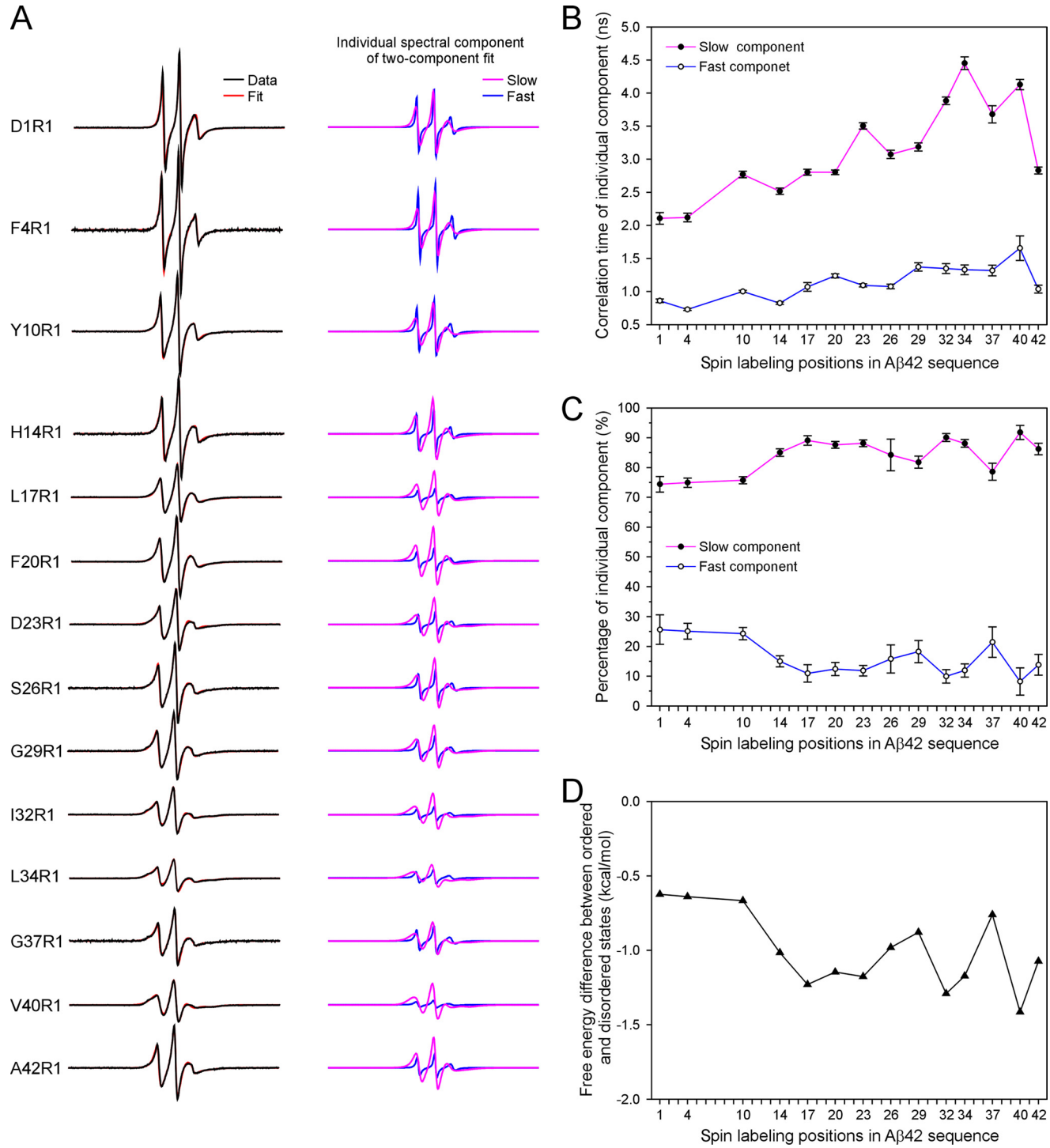

FIGURE 3. **Residue-specific EPR mobility analysis for spin-labeled Aβ42 globulomers.** *A*, the experimental EPR spectra of 25% labeled Aβ42 globulomers, which consist of spin-labeled and wild-type Aβ42 at 1:3 molar ratio, are shown in *black*. The best nonlinear least squares fits from spectral simulations are shown in *red*. All the fits contain two spectral components: a slow component (*magenta*) and a fast component (*blue*). *B*, plot of correlation time for the slow and fast components obtained from spectral simulations. *C*, plot of the populations of the fast and slow components from spectral simulations. *D*, residue-level local structural stability calculated using the relative populations of the slow (for structured state) and fast (for disordered state) components. *Error bars* in *B* and *C* indicate fitting errors.

We measured intermolecular distances in Aβ42 globulomers using continuous wave EPR, which is sensitive to distances in the range of 8–20 Å (41). For distance measurements, EPR spectra were collected at 170 K. The EPR spectra are shown in Fig. 5*B*, and the measured distances are shown in Fig. 5*C* (*top panel*). The segment with the shortest distances is located at residues Gly-29–Val-40, with distances of 11.5–12.5 Å. Residues Phe-4–Ser-26 have slightly longer distances in the range of 12.5–13.5 Å. The two terminal residues Asp-1 and Ala-42 give distances >13.5 Å.

The intermolecular distances from EPR provide structural restraints for the intermolecular organization of Aβ42 subunits

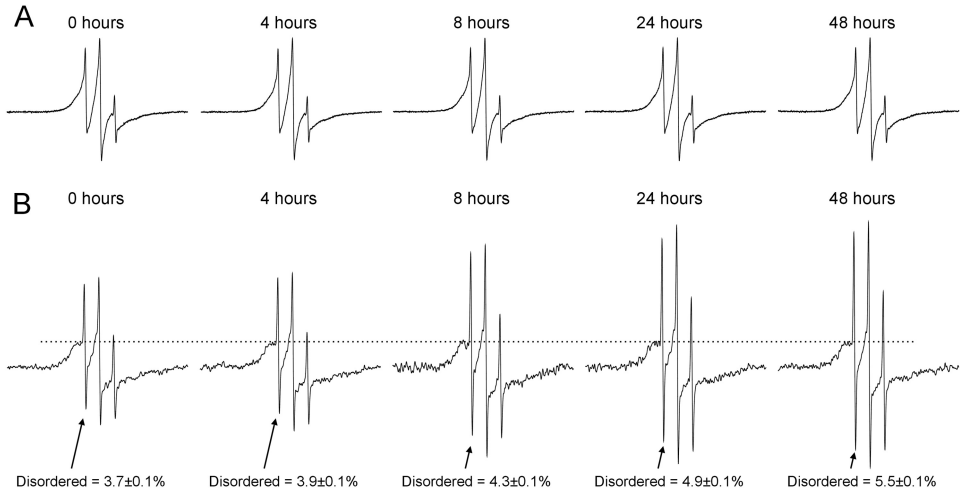

FIGURE 4. **Temporal stability of Aβ42 globulomers.** *A*, EPR spectra of Aβ42 L34R1 globulomers at room temperature in preparation buffer (5 mM phosphate, pH 7.4, 35 mM NaCl, 2% DMSO, and 0.05% SDS). *B*, EPR spectra of Aβ42 L34R1 globulomers at room temperature after 10-fold dilution to cell culture medium, which is ATCC-formulated RPMI 1640 medium with 10% heat-inactivated horse serum and 5% fetal bovine serum. *Dotted line* was drawn to aid comparison of different spectra.

in globulomers. First, Aβ42 globulomers consist of a tightly packed C-terminal region (Gly-29–Val-40) and a loosely packed N-terminal region. Second, the shortest distances observed at residues Gly-29–Val-40 are in the range of 11.5–12.5 Å, suggesting the absence of parallel in-register β-structures. Third, the intermolecular distances for most labeling positions are in a narrow range of 11.5–13.5 Å, suggesting an overall parallel arrangement for the Aβ42 subunits at this spacing. In Fig. 6, we depict four schematic models for the potential arrangement for the C-terminal region (Gly-29–Val-40). In Fig. 6, *A* and *C*, the measured interspin distances correspond to spacing between alternating β-strands within the same β-sheet. In Fig. 6, *B* and *D*, the interspin distances correspond to spacing between two face-to-back packed β-sheets.

From distance analysis, we obtained not only distances in the range of 8–20 Å, but also the population of spin labels at the measured distances. We also obtained population of spin labels at distances >20 Å, which do not contribute to spectral broadening. Fig. 5*C* (*bottom panel*) shows that only ~25–50% of spin labels give rise to the measured distances in the range of 11.5–14.5 Å. The majority of the spin labels are at distances >20 Å (Fig. 5*D*). This information may also be useful in detailed structural modeling studies. For example, in Fig. 6*A*, spin labels on the *green β-strand* would fall into the category of >20 Å.

EPR Studies of Aβ42 Preglobulomers—Previous studies suggest that globulomer formation involves the formation of preglobulomers in 0.2% SDS (13). After a 4-fold dilution of preglobulomers with water, preglobulomers convert to globulomers. Yu *et al.* (35) characterized the preglobulomers and proposed an intermolecular parallel in-register β-sheet model for residues 34–41. Here we also characterized the preglobulomer structures with Aβ42 L34R1. The EPR spectrum of preglobulomers prepared in 0.2% SDS also consists of two spectral components, similar to globulomers (Fig. 7*A*). Superimposition of the preglobulomer and globulomer spectra shows that the major difference between the two spectra is the more pronounced population of the disordered component. The line shape for the ordered component is similar between preglobulomer and globulomer samples, suggesting structural similarity. Because Yu *et al.* (35) characterized the preglobulomers prepared in 1.5% SDS with solution NMR, we also performed EPR measurements at 1.5% SDS. The EPR spectrum of preglobulomers in 1.5% SDS (Fig. 7*B*) is slightly sharper than that in 0.2% SDS, suggesting higher structural flexibility in 1.5% SDS. However, the overall EPR spectral line shape is similar between 0.2 and 1.5% SDS, suggesting overall similar structure for Aβ42 preglobulomers at the two SDS concentrations.

DISCUSSION

Formation of Aβ42 oligomers has been viewed as a key event in the pathogenesis of AD. The structures of Aβ42 oligomers, although essential for rational design of therapeutic agents that target these oligomers, remain elusive. In this work, we provide a systematic investigation into the structure of a toxic Aβ42 oligomer termed globulomer. CD and x-ray powder diffraction data show that Aβ42 globulomers are rich in β-structures (Fig. 1). Side chain mobility studies show increasing structural order from N- to C-terminal regions, with residues Ile-32–Val-40 being the most ordered region (Fig. 3). Intermolecular distance measurements show that side chains at residues Gly-29–Val-40 have an intermolecular spacing of ~11.5–12.5 Å (Fig. 5). Because EPR measures distances between the nitroxide groups, the linking arm between the nitroxide group and the Cα carbon introduces an additional variant when translating distances into structural models. Despite these uncertainties, the intermolecular distances for the C-terminal residues Gly-29–Val-40 are in a range of 11.5–12.5 Å, close to the spacing between alternating β-strands within the same sheet or between adjacent β-sheets.

Although a detailed structural model for Aβ42 globulomers is still beyond reach, the distance measurements provide restraints to assess published computational models. First, the measured distances rule out parallel in-register arrangement in globulomers. Recent studies using FTIR spectroscopy have suggested the existence of antiparallel β-structures in Aβ oligomers prepared using a wide range of protocols (16–24). Some

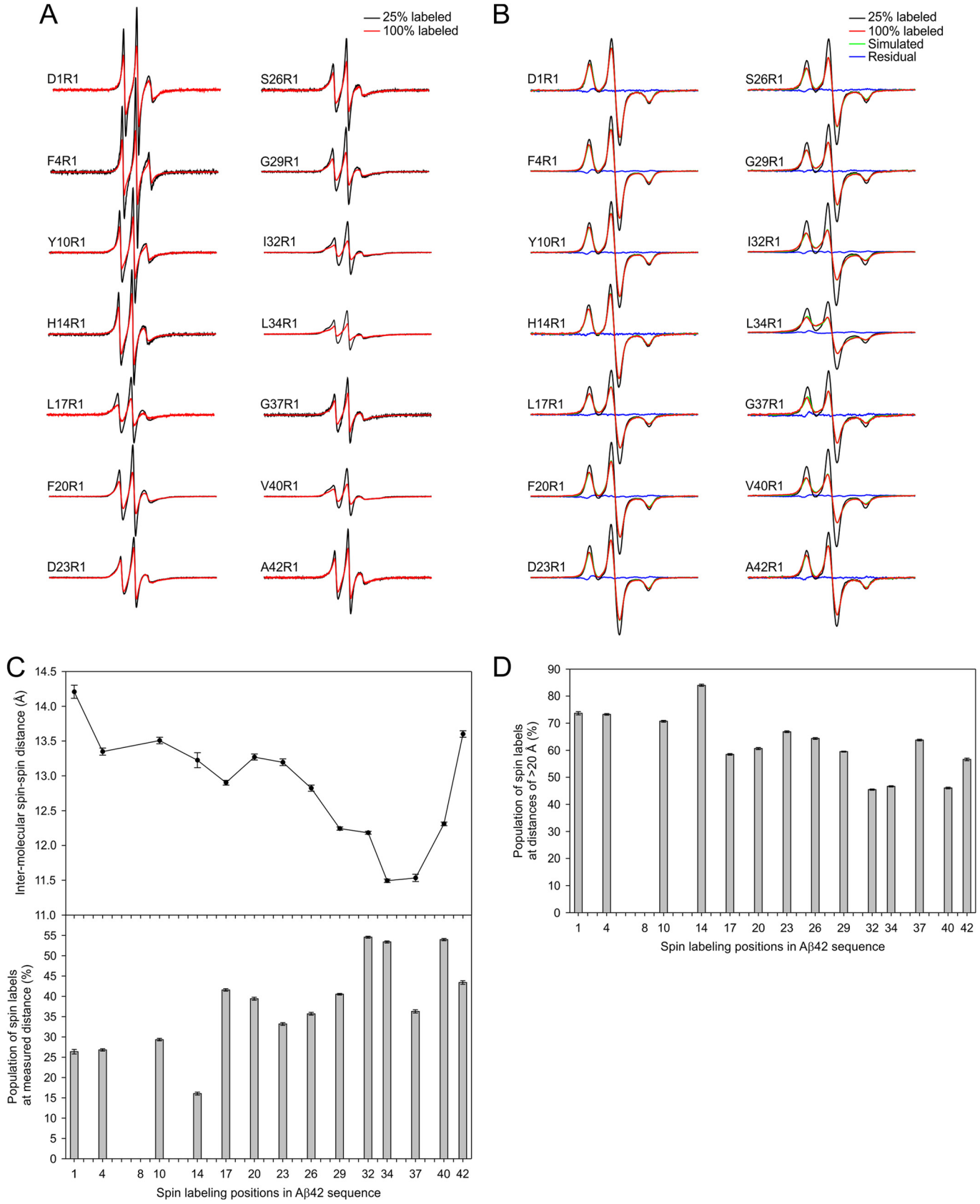

FIGURE 5. **Intermolecular distance measurements for spin-labeled Aβ42 globulomers.** *A*, EPR spectra of 100% labeled oligomers at room temperature show significantly reduced spectral amplitude than 25% labeled samples, suggesting intermolecular dipolar interactions. *B*, EPR spectra of 25 and 100% labeled Aβ42 globulomers at 170 K. Interspin distances are obtained by simulating the 100% labeled spectra. The residual is the difference between simulated spectra and 100% labeled spectra. *C*, plot of intermolecular distance between spin labels and the percentage of spin labels at measured distances. *D*, plot of the populations of spin labels at >20 Å. *Error bars* in *C* and *D* indicate fitting errors.

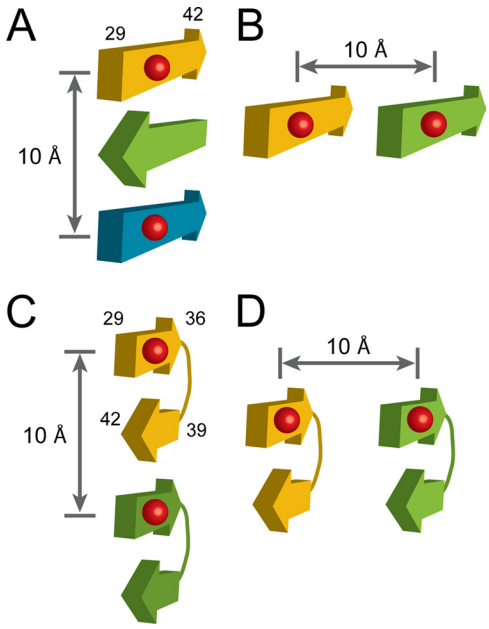

FIGURE 6. **Potential structural origins of measured intermolecular distances for C-terminal residues Gly-29–Ala-42.** *A–D*, different β-strand organizations giving rise to the measured distances at ~10 Å. *Red balls* represent spin labels. *Numbers* in *A* and *C* show approximate residue positions for each β-strand segment. Each model consists of only a minimum repeating unit, which can be extended in either hydrogen-bonding or side chain directions.

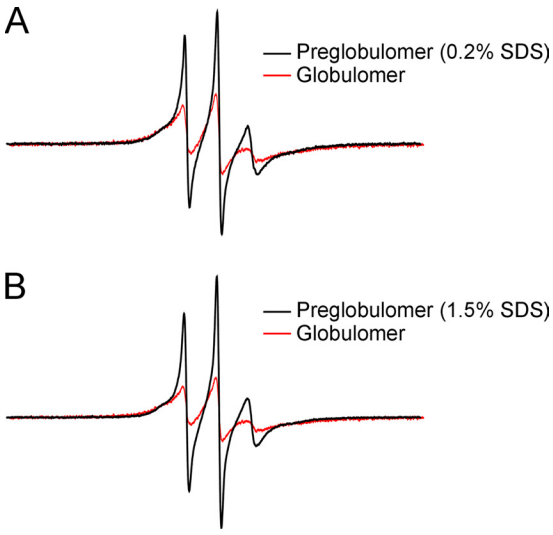

FIGURE 7. **EPR spectra of Aβ42 L34R1 preglobulomers.** *A*, preglobulomers prepared in 0.2% SDS. *B*, preglobulomers prepared in 1.5% SDS.

investigators have questioned whether FTIR is able to definitively distinguish parallel from antiparallel structures in amyloid oligomers (51, 52). The distance measurements strongly support the antiparallel arrangement in Aβ42 globulomers and may put this concern to rest. In computational modeling (53–55), Aβ42 subunits (residues 17–42) are generally modeled as a β-hairpin (56, 57) or a U-shaped strand-turn-strand motif as observed in Aβ fibrils (58). The measured distances are generally in support of the antiparallel structural models in these modeling studies (53–55).

Previously, Yu *et al.* (35) characterized the structures of preglobulomers using solution NMR. Preglobulomers are formed

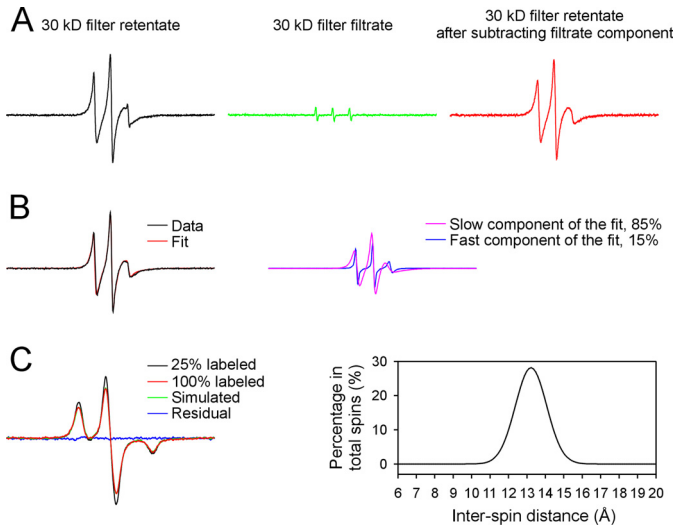

FIGURE 8. **EPR analysis can resolve structural heterogeneity in Aβ oligomers.** *A*, spectral subtraction to isolate the spectral component of interest. *B*, spectral simulations to reveal multiple structural states. *C*, distance analysis to reveal both the distance and the relative population of spin labels at the measured distance.

in a higher concentration of SDS (0.2% *versus* 0.05% for globulomers). NMR data on Aβ42 preglobulomers show that residues 34–41 adopt intermolecular parallel in-register β-sheet structures, similar to those in fibrils. Solution NMR studies were not performed on Aβ42 globulomers due to the large size, but hydrogen exchange studies show that the only highly protected segment in both preglobulomers and globulomers is the C-terminal region (residues 30–42) (35), consistent with EPR data that show higher structural order and closer intermolecular distances in the C-terminal region. The EPR spectra of Aβ42 preglobulomers are similar to those of globulomers (Fig. 7), suggesting similar structural features. The reason for this apparent contradiction between EPR results and the previous NMR studies is not clear and may result from structural polymorphism commonly observed for Aβ oligomers.

The findings here demonstrate that EPR studies can resolve structurally heterogeneous states. One property of Aβ oligomer preparations that makes it challenging to do high-resolution structural studies is the sample heterogeneity. This work has demonstrated several advantages of EPR in obtaining structural information from structurally heterogeneous samples. First, spectral subtraction can be used to obtain the EPR spectrum of pure oligomers by subtracting a spectral component with known line shape (Fig. 8*A*). Using a 30-kDa molecular mass cut-off filter, we separated Aβ42 globulomers into two fractions. The 30-kDa filter filtrate contains disordered Aβ monomers based on the sharp EPR lines. The EPR spectra of the pure high molecular mass species can be obtained by subtracting the 30-kDa filter filtrate spectra from the retentate spectra (Fig. 8*A*). Second, multiple spectral components can be resolved using spectral simulations, which give dynamic parameters and populations of each component (Fig. 8*B*). Third, in distance measurements, the distance and its population can be determined simultaneously using spectral fitting (Fig. 8*C*). Furthermore, EPR has the ability to measure a wide range of distances (8–70 Å). These advantages make site-directed spin labeling

EPR an extremely powerful tool in the structural studies of the heterogeneous amyloid oligomers of Aβ and other proteins.

Acknowledgments—We thank Dr. David Eisenberg for use of the x-ray facility, Sam Ngo for preparation of Aβ proteins, and Dr. Christian Altenbach and Dr. Wayne Hubbell for providing EPR analysis programs.

REFERENCES

1. Selkoe, D. J. (2011) Alzheimer's disease. *Cold Spring Harb. Perspect. Biol.* **3,** a004457
2. De Strooper, B. (2010) Proteases and proteolysis in Alzheimer disease: a multifactorial view on the disease process. *Physiol. Rev.* **90,** 465–494
3. Iwatsubo, T., Odaka, A., Suzuki, N., Mizusawa, H., Nukina, N., and Ihara, Y. (1994) Visualization of Aβ42(43) and Aβ40 in senile plaques with end-specific Aβ monoclonals: Evidence that an initially deposited species is Aβ42(43). *Neuron* **13,** 45–53
4. Hardy, J., and Selkoe, D. J. (2002) The amyloid hypothesis of Alzheimer's disease: Progress and problems on the road to therapeutics. *Science* **297,** 353–356
5. McLean, C. A., Cherny, R. A., Fraser, F. W., Fuller, S. J., Smith, M. J., Beyreuther, K., Bush, A. I., and Masters, C. L. (1999) Soluble pool of Aβ amyloid as a determinant of severity of neurodegeneration in Alzheimer's disease. *Ann. Neurol.* **46,** 860–866
6. Bemporad, F., and Chiti, F. (2012) Protein misfolded oligomers: experimental approaches, mechanism of formation, and structure-toxicity relationships. *Chem. Biol.* **19,** 315–327
7. Kawarabayashi, T., Shoji, M., Younkin, L. H., Wen-Lang, L., Dickson, D. W., Murakami, T., Matsubara, E., Abe, K., Ashe, K. H., and Younkin, S. G. (2004) Dimeric amyloid β protein rapidly accumulates in lipid rafts followed by apolipoprotein E and phosphorylated Tau accumulation in the Tg2576 mouse model of Alzheimer's disease. *J. Neurosci.* **24,** 3801–3809
8. Shankar, G. M., Li, S., Mehta, T. H., Garcia-Munoz, A., Shepardson, N. E., Smith, I., Brett, F. M., Farrell, M. A., Rowan, M. J., Lemere, C. A., Regan, C. M., Walsh, D. M., Sabatini, B. L., and Selkoe, D. J. (2008) Amyloid-β protein dimers isolated directly from Alzheimer's brains impair synaptic plasticity and memory. *Nat. Med.* **14,** 837–842
9. Lesné, S., Koh, M. T., Kotilinek, L., Kayed, R., Glabe, C. G., Yang, A., Gallagher, M., and Ashe, K. H. (2006) A specific amyloid-β protein assembly in the brain impairs memory. *Nature* **440,** 352–357
10. Roychaudhuri, R., Yang, M., Hoshi, M. M., and Teplow, D. B. (2009) Amyloid β-protein assembly and Alzheimer disease. *J. Biol. Chem.* **284,** 4749–4753
11. Benilova, I., Karran, E., and De Strooper, B. (2012) The toxic Aβ oligomer and Alzheimer's disease: an emperor in need of clothes. *Nat. Neurosci.* **15,** 349–357
12. Lambert, M. P., Barlow, A. K., Chromy, B. A., Edwards, C., Freed, R., Liosatos, M., Morgan, T. E., Rozovsky, I., Trommer, B., Viola, K. L., Wals, P., Zhang, C., Finch, C. E., Krafft, G. A., and Klein, W. L. (1998) Diffusible, nonfibrillar ligands derived from $A\beta_{1-42}$ are potent central nervous system neurotoxins. *Proc. Natl. Acad. Sci. U.S.A.* **95,** 6448–6453
13. Barghorn, S., Nimmrich, V., Striebinger, A., Krantz, C., Keller, P., Janson, B., Bahr, M., Schmidt, M., Bitner, R. S., Harlan, J., Barlow, E., Ebert, U., and Hillen, H. (2005) Globular amyloid β-peptide$_{1-42}$ oligomer – a homogenous and stable neuropathological protein in Alzheimer's disease. *J. Neurochem.* **95,** 834–847
14. Glabe, C. G. (2008) Structural classification of toxic amyloid oligomers. *J. Biol. Chem.* **283,** 29639–29643
15. Hoshi, M., Sato, M., Matsumoto, S., Noguchi, A., Yasutake, K., Yoshida, N., and Sato, K. (2003) Spherical aggregates of β-amyloid (amylospheroid) show high neurotoxicity and activate Tau protein kinase I/glycogen synthase kinase-3β. *Proc. Natl. Acad. Sci. U.S.A.* **100,** 6370–6375
16. Cerf, E., Sarroukh, R., Tamamizu-Kato, S., Breydo, L., Derclaye, S., Dufrêne, Y. F., Narayanaswami, V., Goormaghtigh, E., Ruysschaert, J. M., and Raussens, V. (2009) Antiparallel β-sheet: a signature structure of the oligomeric amyloid β-peptide. *Biochem. J.* **421,** 415–423
17. Eckert, A., Hauptmann, S., Scherping, I., Meinhardt, J., Rhein, V., Dröse, S., Brandt, U., Fändrich, M., Müller, W. E., and Götz, J. (2008) Oligomeric and fibrillar species of β-amyloid (Aβ42) both impair mitochondrial function in P301L Tau transgenic mice. *J. Mol. Med.* **86,** 1255–1267
18. Morgado, I., Wieligmann, K., Bereza, M., Rönicke, R., Meinhardt, K., Annamalai, K., Baumann, M., Wacker, J., Hortschansky, P., Malešević, M., Parthier, C., Mawrin, C., Schiene-Fischer, C., Reymann, K. G., Stubbs, M. T., Balbach, J., Görlach, M., Horn, U., and Fändrich, M. (2012) Molecular basis of β-amyloid oligomer recognition with a conformational antibody fragment. *Proc. Natl. Acad. Sci. U.S.A.* **109,** 12503–12508
19. Habicht, G., Haupt, C., Friedrich, R. P., Hortschansky, P., Sachse, C., Meinhardt, J., Wieligmann, K., Gellermann, G. P., Brodhun, M., Götz, J., Halbhuber, K. J., Röcken, C., Horn, U., and Fändrich, M. (2007) Directed selection of a conformational antibody domain that prevents mature amyloid fibril formation by stabilizing Aβ protofibrils. *Proc. Natl. Acad. Sci. U.S.A.* **104,** 19232–19237
20. Ahmed, M., Davis, J., Aucoin, D., Sato, T., Ahuja, S., Aimoto, S., Elliott, J. I., Van Nostrand, W. E., and Smith, S. O. (2010) Structural conversion of neurotoxic amyloid-β(1–42) oligomers to fibrils. *Nat. Struct. Mol. Biol.* **17,** 561–567
21. Stroud, J. C., Liu, C., Teng, P. K., and Eisenberg, D. (2012) Toxic fibrillar oligomers of amyloid-β have cross-β structure. *Proc. Natl. Acad. Sci. U.S.A.* **109,** 7717–7722
22. Sandberg, A., Luheshi, L. M., Söllvander, S., Pereira de Barros, T., Macao, B., Knowles, T. P., Biverstål, H., Lendel, C., Ekholm-Petterson, F., Dubnovitsky, A., Lannfelt, L., Dobson, C. M., and Härd, T. (2010) Stabilization of neurotoxic Alzheimer amyloid-β oligomers by protein engineering. *Proc. Natl. Acad. Sci. U.S.A.* **107,** 15595–15600
23. Sarroukh, R., Cerf, E., Derclaye, S., Dufrêne, Y. F., Goormaghtigh, E., Ruysschaert, J. M., and Raussens, V. (2011) Transformation of amyloid β(1–40) oligomers into fibrils is characterized by a major change in secondary structure. *Cell. Mol. Life Sci.* **68,** 1429–1438
24. Vandersteen, A., Hubin, E., Sarroukh, R., De Baets, G., Schymkowitz, J., Rousseau, F., Subramaniam, V., Raussens, V., Wenschuh, H., Wildemann, D., and Broersen, K. (2012) A comparative analysis of the aggregation behavior of amyloid-β peptide variants. *FEBS Lett.* **586,** 4088–4093
25. Liu, C., Sawaya, M. R., Cheng, P. N., Zheng, J., Nowick, J. S., and Eisenberg, D. (2011) Characteristics of amyloid-related oligomers revealed by crystal structures of macrocyclic β-sheet mimics. *J. Am. Chem. Soc.* **133,** 6736–6744
26. Laganowsky, A., Liu, C., Sawaya, M. R., Whitelegge, J. P., Park, J., Zhao, M., Pensalfini, A., Soriaga, A. B., Landau, M., Teng, P. K., Cascio, D., Glabe, C., and Eisenberg, D. (2012) Atomic view of a toxic amyloid small oligomer. *Science* **335,** 1228–1231
27. Margittai, M., and Langen, R. (2008) Fibrils with parallel in-register structure constitute a major class of amyloid fibrils: molecular insights from electron paramagnetic resonance spectroscopy. *Q. Rev. Biophys.* **41,** 265–297
28. Agopian, A., and Guo, Z. (2012) Structural origin of polymorphism for Alzheimer's amyloid-β fibrils. *Biochem. J.* **447,** 43–50
29. Hubbell, W. L., Cafiso, D. S., and Altenbach, C. (2000) Identifying conformational changes with site-directed spin labeling. *Nat. Struct. Biol.* **7,** 735–739
30. Fanucci, G. E., and Cafiso, D. S. (2006) Recent advances and applications of site-directed spin labeling. *Curr. Opin. Struct. Biol.* **16,** 644–653
31. McHaourab, H. S., Steed, P. R., and Kazmier, K. (2011) Toward the fourth dimension of membrane protein structure: insight into dynamics from spin-labeling EPR spectroscopy. *Structure* **19,** 1549–1561
32. Gellermann, G. P., Byrnes, H., Striebinger, A., Ullrich, K., Mueller, R., Hillen, H., and Barghorn, S. (2008) Aβ-globulomers are formed independently of the fibril pathway. *Neurobiol Dis* **30,** 212–220
33. Hillen, H., Barghorn, S., Striebinger, A., Labkovsky, B., Müller, R., Nimmrich, V., Nolte, M. W., Perez-Cruz, C., van der Auwera, I., van Leuven, F., van Gaalen, M., Bespalov, A. Y., Schoemaker, H., Sullivan, J. P., and Ebert, U. (2010) Generation and therapeutic efficacy of highly oligomer-specific β-amyloid antibodies. *J. Neurosci.* **30,** 10369–10379
34. Nimmrich, V., Grimm, C., Draguhn, A., Barghorn, S., Lehmann, A.,

Schoemaker, H., Hillen, H., Gross, G., Ebert, U., and Bruehl, C. (2008) Amyloid β oligomers (Aβ(1–42) globulomer) suppress spontaneous synaptic activity by inhibition of P/Q-type calcium currents. *J. Neurosci.* **28,** 788–797

35. Yu, L., Edalji, R., Harlan, J. E., Holzman, T. F., Lopez, A. P., Labkovsky, B., Hillen, H., Barghorn, S., Ebert, U., Richardson, P. L., Miesbauer, L., Solomon, L., Bartley, D., Walter, K., Johnson, R. W., Hajduk, P. J., and Olejniczak, E. T. (2009) Structural characterization of a soluble amyloid β-peptide oligomer. *Biochemistry* **48,** 1870–1877
36. Shahnawaz, M., Thapa, A., and Park, I. S. (2007) Stable activity of a deubiquitylating enzyme (Usp2-cc) in the presence of high concentrations of urea and its application to purify aggregation-prone peptides. *Biochem. Biophys. Res. Commun.* **359,** 801–805
37. Baker, R. T., Catanzariti, A. M., Karunasekara, Y., Soboleva, T. A., Sharwood, R., Whitney, S., and Board, P. G. (2005) Using deubiquitylating enzymes as research tools. *Methods Enzymol.* **398,** 540–554
38. Ngo, S., and Guo, Z. (2011) Key residues for the oligomerization of Aβ42 protein in Alzheimer's disease. *Biochem. Biophys. Res. Commun.* **414,** 512–516
39. Schneider, D. J., and Freed, J. H. (1989) Calculating slow motional magnetic resonance specta. in *Spin Labeling: Theory and Applications* (Berliner, L. J., and Reuben, J., eds) pp. 1–76, Plenum Press, New York
40. Budil, D. E., Lee, S., Saxena, S., and Freed, J. H. (1996) Nonlinear-least-squares analysis of slow-motion EPR spectra in one and two dimensions using a modified Levenberg-Marquardt algorithm. *J. Magn. Reson.* **120,** 155–189
41. Altenbach, C., Oh, K. J., Trabanino, R. J., Hideg, K., and Hubbell, W. L. (2001) Estimation of inter-residue distances in spin labeled proteins at physiological temperatures: experimental strategies and practical limitations. *Biochemistry* **40,** 15471–15482
42. Yamamoto, N., Hasegawa, K., Matsuzaki, K., Naiki, H., and Yanagisawa, K. (2004) Environment- and mutation-dependent aggregation behavior of Alzheimer amyloid β-protein. *J. Neurochem.* **90,** 62–69
43. Veluraja, K., Vennila, K. N., Umamakeshvari, K., Jasmine, A., and Velmurugan, D. (2011) Structural investigation of porcine stomach mucin by X-ray fiber diffraction and homology modeling. *Biochem. Biophys. Res. Commun.* **406,** 570–573
44. López, C. J., Oga, S., and Hubbell, W. L. (2012) Mapping molecular flexibility of proteins with site-directed spin labeling: a case study of myoglobin. *Biochemistry* **51,** 6568–6583
45. Columbus, L., and Hubbell, W. L. (2002) A new spin on protein dynamics. *Trends Biochem. Sci.* **27,** 288–295
46. Ngo, S., Chiang, V., Ho, E., Le, L., and Guo, Z. (2012) Prion domain of yeast Ure2 protein adopts a completely disordered structure: a solid-support EPR study. *PLoS One* **7,** e47248
47. Gu, L., Ngo, S., and Guo, Z. (2012) Solid-support EPR studies of Aβ40 monomers reveal a structured state with three ordered segments. *J. Biol. Chem.* **287,** 9081–9089
48. Cunningham, T. F., McGoff, M. S., Sengupta, I., Jaroniec, C. P., Horne, W. S., and Saxena, S. (2012) High-resolution structure of a protein spin-label in a solvent-exposed β-sheet and comparison with DEER spectroscopy. *Biochemistry* **51,** 6350–6359
49. Lietzow, M. A., and Hubbell, W. L. (2004) Motion of spin label side chains in cellular retinol-binding protein: correlation with structure and nearest-neighbor interactions in an antiparallel β-sheet. *Biochemistry* **43,** 3137–3151
50. Guo, Z., Cascio, D., Hideg, K., Kálái, T., and Hubbell, W. L. (2007) Structural determinants of nitroxide motion in spin-labeled proteins: Tertiary contact and solvent-inaccessible sites in helix G of T4 lysozyme. *Protein Sci.* **16,** 1069–1086
51. Zandomeneghi, G., Krebs, M. R. H., McCammon, M. G., and Fändrich, M. (2004) FTIR reveals structural differences between native β-sheet proteins and amyloid fibrils. *Protein Sci.* **13,** 3314–3321
52. Barth, A., and Zscherp, C. (2002) What vibrations tell us about proteins. *Q. Rev. Biophys.* **35,** 369–430
53. Shafrir, Y., Durell, S. R., Anishkin, A., and Guy, H. R. (2010) β-Barrel models of soluble amyloid β oligomers and annular protofibrils. *Proteins* **78,** 3458–3472
54. Ma, B., and Nussinov, R. (2010) Polymorphic C-terminal β-sheet interactions determine the formation of fibril or amyloid β-derived diffusible ligand-like globulomer for the Alzheimer Aβ42 dodecamer. *J. Biol. Chem.* **285,** 37102–37110
55. Ma, B., and Nussinov, R. (2011) Polymorphic triple β-sheet structures contribute to amide hydrogen/deuterium (H/D) exchange protection in the Alzheimer amyloid β42 peptide. *J. Biol. Chem.* **286,** 34244–34253
56. Streltsov, V. A., Varghese, J. N., Masters, C. L., and Nuttall, S. D. (2011) Crystal structure of the amyloid-β p3 fragment provides a model for oligomer formation in Alzheimer's disease. *J. Neurosci.* **31,** 1419–1426
57. Hoyer, W., Grönwall, C., Jonsson, A., Ståhl, S., and Härd, T. (2008) Stabilization of a β-hairpin in monomeric Alzheimer's amyloid-β peptide inhibits amyloid formation. *Proc. Natl. Acad. Sci. U.S.A.* **105,** 5099–5104
58. Tycko, R. (2011) Solid-state NMR studies of amyloid fibril structure. *Annu. Rev. Phys. Chem.* **62,** 279–299
59. Columbus, L., Kálai, T., Jekö, J., Hideg, K., and Hubbell, W. L. (2001) Molecular motion of spin labeled side chains in α-helices: analysis by variation of side chain structure. *Biochemistry* **40,** 3828–3846